ELSEVIER

PII S0142-9612(96)00022-1

Biomaterials 17 (1996) 1975–1980

0142-9612/96/$15.00

Effect of low-intensity ultrasound upon biofilm structure from confocal scanning laser microscopy observation

Zhen Qian*, Paul Stoodley† and William G. Pitt*

*Chemical Engineering Department, Brigham Young University, Provo, UT 84602, USA; †Center for Biofilm Engineering, Montana State University, Bozeman, MT 59717, USA

Ultrasonic irradiation at 500 kHz and 10 mW cm^{-2} of a 24 h old biofilm of *P. aeruginosa* enhanced the killing of bacteria by gentamicin. To determine whether this bioacoustic effect was caused by ultrasonic-induced changes in the biofilm morphology (biofilm breakup or disruption), the biofilms were examined by confocal scanning laser microscopy (CSLM). Such disruption would be undesirable in the possible ultrasonic treatment of implant infections. The CSLM results showed that the biofilm is a partial monolayer of cells with occasional aggregates of cells, non-cellular materials and extracellular spaces. The aggregates contained large amounts of exopolysaccharide. The structure of biofilm was not changed when the biofilm was exposed to continuous ultrasound at 500 kHz and 10 mW cm^{-2}, the same irradiation parameters that increased cell killing by nearly two orders of magnitude. The observation that low-intensity ultrasound does not disrupt biofilm or disperse the bacteria has significance in the possible use of ultrasound to enhance the action of antibiotics against biofilms. © 1996 Elsevier Science Limited.

Keywords: Confocal scanning laser microscopy, ultrasound, biofilm, Pseudomonas aeruginosa, bioacoustic effect

Received 8 November 1995; accepted 5 February 1996

Implanted medical devices are occasionally colonized by bacterial biofilms, resulting in patient suffering and additional surgery for removal or replacement of the devices[1]. Once a biofilm infection is established, it is extremely difficult, if not impossible, to eliminate the infection by antibiotic therapy alone. The concentrations of antibiotic needed to completely eradicate a bacterial biofilm on a polymeric or metal substrate are reported to be 500–5,000 times higher than those that kill planktonic bacteria of the same organism[2]. It has been hypothesized that this inherent resistance is attributed to diffusion limitations[3–6] and/or physiological properties of biofilm sequestered bacteria[7–11].

Researchers in our lab are studying the synergistic effect of ultrasound and antibiotics (the bioacoustic effect) to kill bacteria. Planktonic suspensions of *P. aeruginosa* were several times more sensitive to low concentrations of gentamicin antibiotic when they were exposed to ultrasound. The ultrasound itself had no deleterious effect on bacteria viability or growth rate at the power levels applied[12,13]. Similar acoustical enhancement of killing was observed for the bacteria of a 24 h old biofilm grown on polyethylene[14]. Several mechanisms have been hypothesized as to the underlying origins of the bioacoustic effect for biofilms. The foremost hypothesis was that the ultrasound enhanced the transport of antibiotics through the biofilm to the surface of the bacterium, or that the ultrasound breaks up the biofilm, thereby exposing more of the bacteria to the antibiotic. Another hypothesis is that ultrasound facilitates the transport of antibiotic through the cell membrane. A third possibility is that ultrasound interferes with biochemical reactions within the bacteria.

The objective of this work was to use confocal scanning laser microscopy (CSLM) to examine the structure of biofilm *in situ* and the effect of ultrasound on the biofilm structure, under the same acoustic irradiation that produces enhanced antibiotic killing. CSLM allows the biofilm to be observed under hydrated conditions, thus maintaining structure that is normally altered using conventional fixative techniques[15,16]. Additionally, CSLM enhances visualization of biofilm structure by eliminating the interference from out of focus light[17]. This also allows the specimen to be optically sectioned to reveal the three-dimensional structure, and any changes in that structure that may occur upon ultrasonic treatment.

MATERIALS AND METHODS

Microorganism

Five millilitres of tryptic soy broth (TSB) without glucose (DIFCO, Detroit, MI) were inoculated from a

Correspondence to Dr W.G. Pitt.

frozen culture of *Pseudomonas aeruginosa* (GNRNF-PsA-1) and incubated overnight at 37°C. At 16 h, 1 ml of the culture was transferred to 100 ml of sterile TSB and grown at 37°C for 6 h. This culture was used to initiate the growth of biofilms as described subsequently.

Assessment of the bioacoustic effect

Experiments measuring the acoustically enhanced killing of *P. aeruginosa* by gentamicin have been described in detail elsewhere[14,18]. Briefly, biofilms were grown in TSB on the end of high-density polyethylene (PE) plugs. After 24 h of growth, the biofilms were exposed to 500 kHz ultrasound at 10 mW cm^{-2} and 1 mW cm^{-2} intensity, with and without 12 μg ml^{-1} gentamicin sulphate. Control experiments without ultrasound were done at the same time. After 2 h insonation, the biofilms were removed from the plugs and the number of viable cells was determined by standard plate counting techniques.

CSLM flow cell and biofilm development

The confocal experiment employed a novel flow cell in which a confocal microscope could view the biofilm during ultrasonic irradiation. The bottom section of the polycarbonate flow cell contained a shallow rectangular chamber through which the bacteria suspension and nutrient were pumped (*Figure 1*). A 9.5 mm diameter hole was drilled in the middle of the bottom section and a glass cover slip was sealed over the hole. The upper polycarbonate section of the flow cell contained a rectangular chamber and a hole with gaskets that accommodated a focussed ultrasonic transducer. The transmitting end of the transducer was positioned flush with the inner surface. There were also fluid entry and exit ports on the top piece through which TSB was pumped to fill the chamber. A polypropylene film (EX-29, Exxon, Marlin, PA) which allows ultrasound to penetrate with minimal reflection and absorption was placed between the two sections and separated the two chambers. The distance between the end of the transducer and the glass cover slip was 17 mm and the area of the glass cover slip exposed to ultrasound was 17.8 mm^2. The design of this double chamber reduced the residence time of TSB in the lower compartment of the flow cell and allowed the transducer to be moved from one flow cell to another without compromising the sterility of the lower chamber.

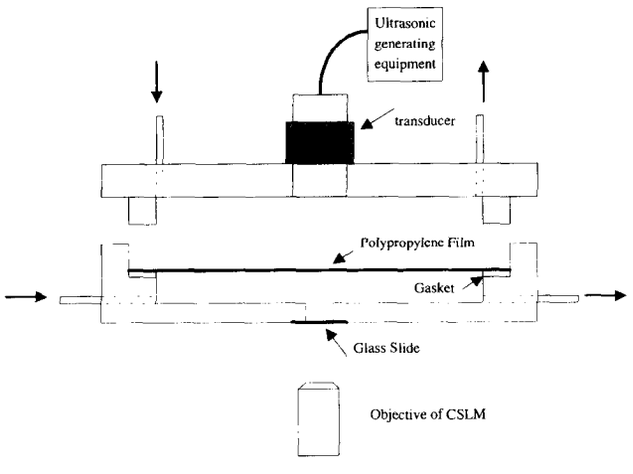

Figure 1 Schematic diagram of the double-chambered flow cell.

The biofilm was grown by pumping the 6 h old bacteria suspension through the lower chamber for 1 h, and then pumping sterile, aerated TSB for 24 h at a rate of 1 ml min^{-1}. After 24 h of growth at 37°C, the biofilms were viewed with CSLM.

Confocal scanning laser microscope and image analysis

A Bio-Rad MRC 600 confocal scanning laser microscope in conjunction with an Inverted Olympus IMT2 Microscope was used for this study. The biofilm was imaged with a 50× ultra-long working distance objective with a zoom using the Bio-Rad COMOS operating software. The biofilm was stained with ethidium bromide (a nucleic acid stain) prior to observation. Images were captured using the COMOS software and quantitatively analysed using NIH Image Software (NIH, Washington, DC).

Ultrasound source

For both the CSLM experiment and the bioacoustic killing experiment, the 500 kHz ultrasound was delivered by a focussed ultrasonic immersion transducer (V318-SU, Panametrics, Waltham, MA). A function generator (Hewlett Packard 3312A) produced a 500 kHz continuous sinusoidal wave, and then an RF amplifier (Model 240L, ENI, Rochester, NY) amplified the wave to produce a power density of 10 mW cm^{-2} at the surface of the glass cover slip or the surface of the PE plug. An oscilloscope was used to monitor the frequency, waveform and power density of the ultrasound.

The power density of the transducer was calibrated as a function of applied voltage in a separate experiment using the radiation force technique[19,20]. The calibration was performed by suspending a hollow aluminium target from below the pan of a Mettler MT5 microbalance (Mettler-Toledo, Hightstown, NJ). The target was suspended with polyethylene fibres (Spectra 1000, Allied Signal). The balance and target assembly were enclosed to shield them from drafts. The target had dimensions of 40 mm × 40 mm × 6.0 mm and was bent in the centre at a 136° angle, giving a projected area of 14.8 cm^2. The balance and target were suspended over a 20 gallon tank filled with water, with the target about 5 cm below the water surface. The 500 kHz transducer was positioned 3.8 cm (twice the focal length of the transducer) directly above the target with the axis of the transducer pointing vertically downward to the centre of the target. Acoustically absorbent material was placed a few centimetres from the sides of the target so that waves reflected from the target would be absorbed instead of reflecting back to the target and interfering with the calibration. The power emitted by the transducer was calculated from the following equation

$$P = I_{ave} A = Fc/(2\cos^2\theta)$$

where I_{ave} is the average insonation intensity, A is the ultrasonic beam cross-section area, F is the downward force on the target (measured by the balance), c is the ultrasonic wave velocity, and θ is the deflection angle of the reflected beam (22°). The area on the target irradiated by the ultrasound was estimated to be a circle of 19 mm diameter. Thus the target intercepted all of the incident insonation. The calculated power is therefore a spatial average and temporal average.

A calibration of applied voltage versus emitted power was constructed by measuring the power at several voltage levels. The precision of calibration was estimated to be ± 15%. The average power density in the experiments was determined by dividing the emitted power by the cross-sectional area of the beam, which was calculated from the focal length and area of the face of the transducer.

Experimental procedure

After 24 h of bacterial growth, the flow cell and its flow system were mounted on the inverted microscope stage, making the biofilm on the glass cover slip accessible for *in situ* CSLM examination. Then the ultrasonic transducer was inserted and the upper chamber was filled with TSB. Ethidium bromide (0.2 ppm final concentration) was pumped into the flow cell for 1 h. Then images of biofilm at various locations on the cover slip were collected. When a particularly large or interesting biofilm structure was found, the ultrasound was switched on and several CSLM images were collected at regular time intervals.

RESULTS

Acoustically enhanced killing

Figure 2 shows the mean viability (and 95% confidence intervals) of the bacteria in the biofilm after 2 h of exposure to the ultrasound alone, the gentamicin alone, and to both gentamicin and ultrasound. Data from experiments at both 10 and 1 mW cm^{-2} are shown. This data represents a large number of experiments: 33 experiments without ultrasound (control and gentamicin only), 22 experiments at 10 mW cm^{-2}, and 11 experiments at 1 mW cm^{-2}. The second bar in each figure shows the viable concentration after 2 h of exposure to the ultrasound. At both power densities, there are no significant differences ($P > 0.05$) between these and the control populations. This low power ultrasonication is apparently insufficient to either remove cells from the PE surface, or to kill the cells. The third bar in each figure indicates the viable concentration after 2 h exposure to 12 μg ml^{-1} gentamicin without ultrasound. Under these conditions, 90% of the cells were killed. This is consistent with previous reports of antibiotic action on biofilms and suspensions of *P. aeruginosa*[12–14, 18, 20].

The fourth bar in the figure shows the viability of the biofilm after the combination of gentamicin and ultrasound. At both power densities, there is a significant ($P < 0.05$) decrease compared to the control. Comparing the 3rd and 4th bars, there is additional killing beyond that of gentamicin alone, and this decrease is statistically significant ($P < 0.05$) for the higher power density. Thus the question arises as to whether the higher power density could have caused increased killing because it disrupted the biofilm structure and exposed more of the bacteria to the gentamicin, or if the killing was increased without disrupting the biofilm structure.

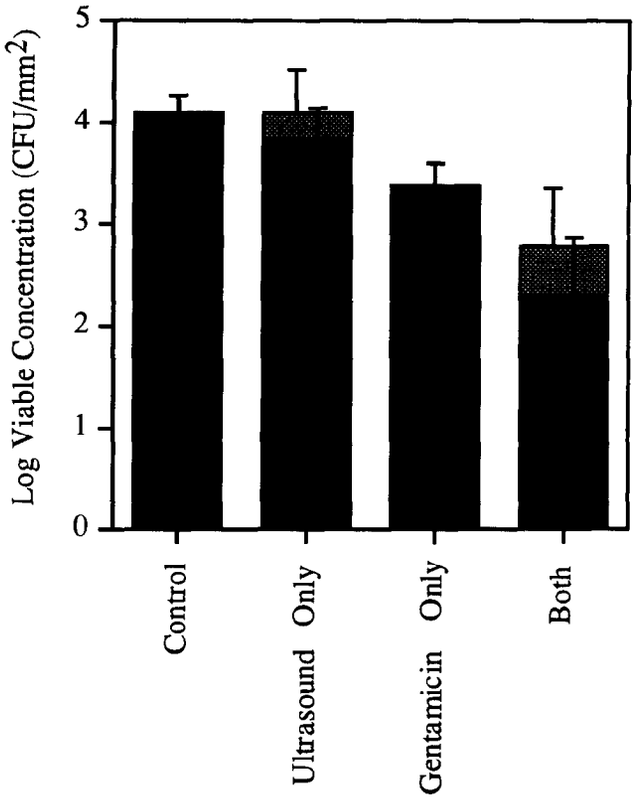

Figure 2 Mean and 95% confidence intervals of the $\log_{10}$ of the viable concentration of *P. aeruginosa* from biofilms after 2 h exposure to 500 kHz ultrasound, 12 μg ml^{-1} gentamicin, or both ultrasound and gentamicin. The solid black bars and grey bars represent ultrasonic exposure at 10 mW cm^{-2} and 1 mW cm^{-2}, respectively.

Structure of the biofilm

The CSLM observations revealed that most of the test surface was covered with a submonolayer distribution of cells. Large cell aggregates, or biofilm structures, occupied less than 10% of the surface. The large aggregates were optically sectioned by collecting vertical thin sections perpendicular to the glass surface. Some of the biomass aggregates had complex three-dimensional structures, and the nucleic acid stain revealed individual cells supported in an extracellular matrix. The individual cells were 2–3 μm rods and were distributed within the biomass at spacings of similar magnitude. *Figure 3* shows a 3D reconstruction of a toroidal-shaped biofilm structure. The dark spots represent the bacterial cells, and the nebulous grey material is assumed to be exopolysaccharide. The

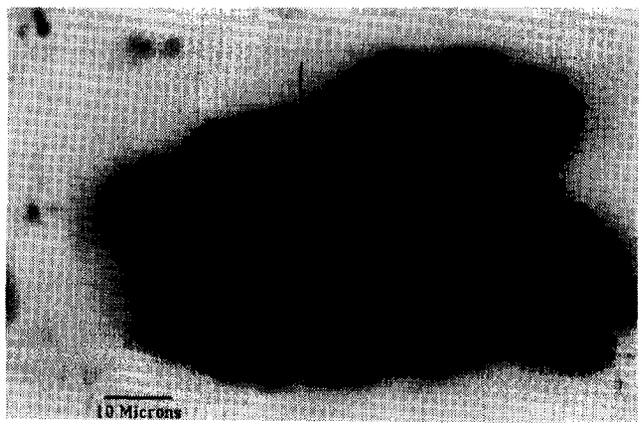

Figure 3 3D reconstruction of a toroidal biofilm aggregate in a 24 h biofilm. The image is 100 × 62 micrometres (width × height). The dark particles are cells stained with a DNA stain. The lighter grey material is exopolysaccharide matrix. The arrow points to an individual cell.

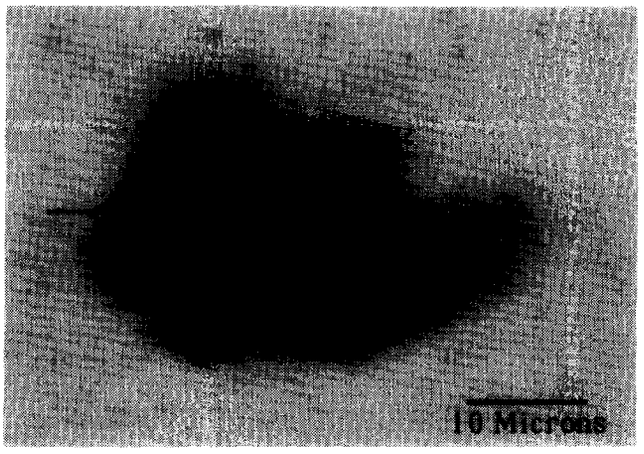

Figure 4 Images of a biofilm aggregate before after exposure to 500 kHz ultrasound for 35 min. The image is 55 × 36 micrometres. See *Figure 3* caption for details.

figure illustrates the form and arrangement of cells within the biofilm and reveals the presence of large amounts of extracellular material and relatively large distances between cells.

The effect of ultrasound on the structure of the biofilm

Figure 4 depicts a cross-section of a different biofilm structure after exposure to 500 kHz ultrasound for 35 min. The structure looked identical to this image before ultrasonic exposure. However, digital subtraction of the images revealed subtle structural changes. *Figures 5a–c* show subtracted images in which the image before ultrasonication is subtracted from the images at 10, 20 and 35 min of ultrasonic exposure. In these figures, black represents material present that was not present before ultrasonication, and white represents material present before treatment but not at longer times. With increasing time the subtracted images get darker, indicating that some material is present at a longer time that was not present before initiation of ultrasonication. The magnitude of these changes is of the order of 1 μm.

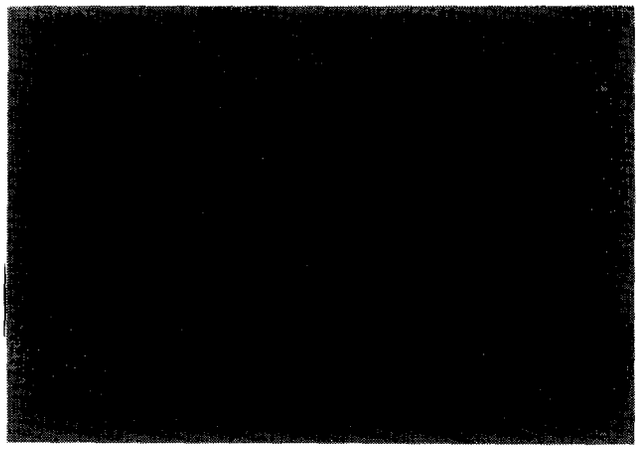

a

b

c

Figure 5 Digital subtraction of the biomass images. **a**, Image at 10 min minus the image before ultrasonication. **b**, Image at 20 min minus the image before ultrasonication. **c**, Image at 35 min minus the image before ultrasonication. The darker shading represents material present at 10, 20 or 35 min that was not present before ultrasonication; the lighter shading represents material present before treatment but not present at later times.

Thus the changes are not due to gross disruption or removal of the biofilm by ultrasound. We postulate that the gradual darkening of these images is due to the natural growth process of the biofilm during the course of the observation.

DISCUSSION

The CSLM provided non-invasive imaging of intact biofilm because the images are not affected by preparatory techniques, and the biofilms do not undergo structural deformation caused by drying, embedding, or sectioning procedures. The images presented above show that a 24 h old biofilm of *P. aeruginosa* appears to be non-uniform in structure, consisting of a sub-monolayer of cells with occasional cell aggregates. The viable cell counts of a 24 h old *P. aeruginosa* biofilm on glass are about 100,000 CFU mm^{-2}. Assuming a projected cell area of 2 square micrometres (2×10^{-12} m^2) and that one cell correlates with one CFU, the calculated surface coverage is about 20%, which is consistent with the CSLM observation of submonolayer coverage. Despite this low coverage in a young biofilm, three-dimensional biomass structures exist. They appear to be highly hydrated and contain large amounts of non-cellular material. We postulate that exopolysaccharide is the major component of these non-cellular materials. These observations corroborate with previous reports that a biofilm is an open system of cells, exopolymeric materials, and extracellular spaces[15,17]. These pores and channels are postulated to facilitate oxygen and other nutrient transport throughout the biofilm[21].

A previously proposed hypothesis as to why the higher power density ultrasound produced more cell killing was that the higher power ultrasound was breaking up the biofilm and allowing antibiotic access to the interior parts of the biofilm. However, these confocal observations show that the application of 10 mW cm^{-2} ultrasound (the power level used in acoustic enhanced killing) did not change the structure of the biofilm or the spatial arrangement of the cells. In fact, the biofilm appeared to grow during the insonation. These findings support the alternative hypothesis that ultrasound does not enhance biofilm killing by disrupting the biofilm. The bioacoustic effect may be related to the enhancement of antibiotic transport through the cell membrane or interference with internal metabolic activity of the bacteria.

The observation that low-power ultrasound does not disrupt the biofilm is significant in the clinical application of this technology to the treatment of implant infections. Since low-intensity ultrasound does not disperse a biofilm, there is minimal concern that ultrasonic treatment of an implant infection would break up and disseminate clusters of biomass to other parts of the body. Further research is ongoing to determine if the combination of ultrasound and antibiotic treatment could be a safe, non-invasive, and non-surgical therapy for treating implant infection.

ACKNOWLEDGEMENTS

Funds for this work were provided by the Whitaker Foundation and the NIH (grant R01 HL52216-01). The confocal laser microscope used in this research was supported by the National Science Foundation (cooperative agreement EEC-8907039) and Montana State University.

REFERENCES

1 Costerton JW, Cheng KJ, Geesey GG, Ladd TI, Nickel JC, Dasgupta M. Bacterial biofilms in nature and disease. *Ann Rev Microbiol* 1987; **41:** 435–464.

2 Khoury AE, Lam L, Ellis B, Costerton JW. Prevention and control of bacterial infections associated with medical devices. *Am Soc Artif Intern Organs J* 1992; **38:** M174–M178.

3 Nicas TI, Iglewski BH. The contribution of exoproducts to virulence of *Pseudomonas aeruginosa*. *Can J Microbiol* 1985; **31:** 387–392.

4 Nichols WW, Dorrington SM, Slack MPE, Walmsley HL. Inhibition of tobramycin diffusion by binding to alginate. *Antimicrob Agents Chemother* 1988; **32:** 518–523.

5 Suci PA, Mittelman MW, Yu FP, Geesey GG. Investigation of ciprofloxacin penetration into *Pseudomonas aeruginosa* biofilms. *Antimicrob Agents Chemother* 1994; **38:** 2125–2133.

6 Wise R. The biofilm glycocalyx as a resistance factor. *J Antimicrob Chemother* 1990; **26:** 1–6.

7 Brown MRW, Allison DG, Gilbert P. Resistance of bacterial biofilms to antibiotics: a growth-rate related effect? *J Antimicrob Chemother* 1988; **22:** 777–783.

8 Brown MRW, Collier PJ, Gilbert P. Influence of growth rate on susceptibility to antimicrobial agents: modification of the cell envelope in batch and continuous culture studies. *Antimicrob Agents Chemother* 1991; **34:** 1632–1628.

9 Gilbert P, Brown MRW. Influence of growth rate and nutrient limitation on the gross cellular composition of Pseudomonas aeruginosa and its resistance to 3- and 4-chlorophenol. *J Bacteriol* 1978; **133:** 1066–1072.

10 Eng RH, Padberg FT, Smith SM, Tan EN, Cherubin CE. Bactericidal effects of antibiotics on slowly growing and nongrowing bacteria. *Antimicrob Agents Chemother* 1991; **35:** 1824–1828.

11 Gilbert P, Brown MRW, Collier PJ. Influence of growth rate on susceptibility to antimicrobial agents: biofilms, cell cycle, dormancy, and stringent response. *Antimicrob Agents Chemother* 1990; **34:** 1865–1868.

12 Pitt WG, McBride MO, Lunceford JK, Roper RJ, Sagers RD. Ultrasonic enhancement of antibiotic action on gram-negative bacteria. *Antimicrob Agents Chemother* 1994; **38:** 2577–2582.

13 Pitt WG, Roper RJ, Sagers RD. The effects of power density on ultrasonic enhancement of antibiotic action on *Pseudomonas aeruginosa*. *Antimicrob Agents Chemother* (in press).

14 Qian Z, Sagers RD, Pitt WG. The effect of ultrasonic frequency upon enhanced killing of *P. aeruginosa* biofilms. *Anna Biomed Eng* (submitted).

15 Lawrence JR, Korber DR, Hoyle BD, Costerton JW, Caldwell DE. Optical sectioning of microbial biofilms. *J Bacteriol* 1991; **173:** 6558–6567.

16 Caldwell DE, Korber DR, Lawrence JR. Confocal laser microscopy and digital image analysis in microbial ecology. In: Marshall KC, ed. *Advances in Microbial Ecology*, Vol. 12. New York: Plenum, 1992: 1–67.

17 de Beer D, Stoodley P, Roe F, Lewandowski Z. Effects of biofilm structures on oxygen distribution and mass transport. *Biotechnol Bioeng* 1994; **43:** 1131–1138.

18 Qian Z. *Antibiotic and Ultrasonic Treatment of Bacterial Biofilm*, M.Sc. Thesis, Brigham Young University, Provo, Utah, USA, 1996.

19 Pederson PC, Christensen DA. Power measurement techniques applied to imaging system. In: Booth N, ed. *Acoustical Holography*. New York: Plenum; 1975: 711–739.

20 Huang C-T, James G, Pitt WG, Stewart PS. Effect of ultrasonic treatment on the efficacy of gentamicin against established *Pseudomonas aeruginosa* biofilm. *Colloids Surfaces B* (in press).

21 Stoodley P, de Beer D, Lewandowski Z. Liquid flow in biofilm systems. *Appl Environ Microbiol* 1994; **60:** 2711–2716.